Electronic Supplementary Material (ESI) for Chemical Communications.

SUPPORTING INFORMATION

Spindle-Like and Telophase-Like Self-Assemblies Mediated by Complementary Nucleobase Molecular Recognition

Mu Wang[a], Bonnie Choi[a], Zhonghe Sun[a], Xiaohu Wei[b], Anchao Feng[*a], San H. Thang[*c]

[a]Beijing Advanced Innovation Center for Soft Matter Science and Engineering; College of Materials Science and Engineering, Beijing University of Chemical Technology, Beijing 100029 China.

[b]State Key Laboratory of Special Functional Waterproof Materials, Beijing Oriental Yuhong Waterproof Technology Co.,Ltd, Beijing 100123, China.

[c]School of Chemistry, Monash University, Clayton Campus, VIC 3800 Australia.

E-mail: fengac@mail.buct.edu.cn, san.thang@monash.edu

Experimental Section

1.1 General Information

All commercially available reagents and solvents were used without further purification except as indicated below. 2,2'-Azobisisobutyronitrile was recrystallized from methanol. *N*-isopropyl acrylamide was recrystallized from *n*-hexane. ^{1}H NMR spectra were recorded on a Bruker Avance III 400 (400 MHz) spectrometer in DMSO-d_6. Gel permeation chromatography (GPC) was performed using a Shimadzu GPC system (using low dispersity polystyrene as standard) equipped with 10 μm mixed columns in series and in line with a 20 A refractive index detector. DMAc was used as eluent at a flow rate of 1 mL/min. Fluorescence experiments were carried out on a Hitachi F-4600 fluorescence spectrophotometer. The excitation wavelength was 339 nm, the excitation slit was 5 nm, and the emission slit was 2.5 nm with a scanning speed of 500 nm/min. UV-vis spectra were recorded on a Hitachi U-3900H UV-vis spectrophotometer. The micromorphology of self-assemblies were observed by a Hitachi HT7700 transmission scanning electron microscopy (TEM). Circular dichroism (CD) spectrum was recorded on a Jasco-810 spectropolarimeter.

1.2 Synthesis of the RAFT Agent-DTTCP

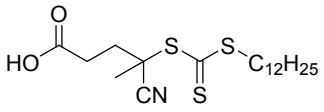

The RAFT agent 4-cyano-4-(dodecylsulfanylthiocarbonyl) sulfanyl pentanoic acid (DTTCP) was prepared according to a literature procedure and ^{1}H NMR data was consistent with those reported previously.[1]

1.3 Synthesis of Nucleobase-containing monomers

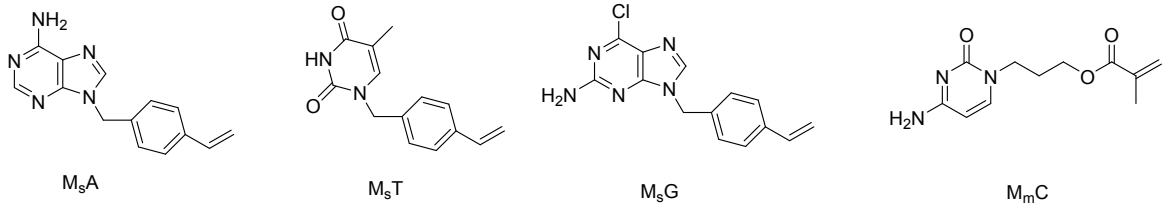

9-(4-vinylbenzyl)adenine (M_sA), 1-(4-vinylbenzyl)thymine (M_sT), 9-(4-vinylbenzyl)guanine (M_sG) and 3-(cytosin-1-yl)propyl methacrylate (M_mC) were prepared according to literature and ^{1}H NMR data was consistent with those reported previously (**Figure S1-S8**).[2-3]

1.4 Synthesis of fluorescent RAFT agent: Danysl-DTTCP and Coumarin-DTTCP

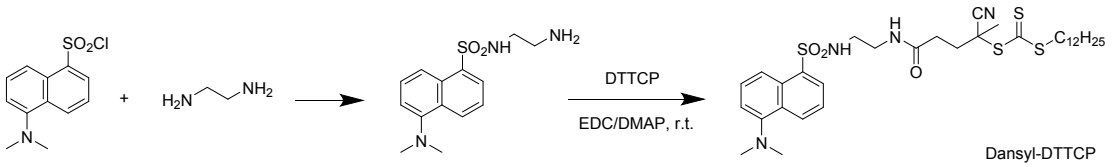

Ethylene diamine (5.6 mL, 82.7 mmol) was suspended in dichloromethane (50 mL) and added dropwise a solution of dansyl chloride (500 mg, 1.8 mmol) in dichloromethane (20 mL) at 0 °C. After addition, the reaction was warmed to room temperature and acidified with 1 mol/L HCl to pH 3. The aqueous layer was extracted with dichloromethane and then separated. The combined organic phases were basified with a 5 mol/L NaOH to pH 9 then extracted with dichloromethane. The combined organic phases were dried over anhydrous sodium sulfate, filtered then evaporated under reduced pressure to provide dansylamine.[4]

Dansylamine (1.47 g, 5.0 mmol) was dissolved in dichloromethane (100 mL), a solution of DTTCP (2.0 g, 5.0 mmol), EDCI (3.83 g, 0.02 mol) and DMAP (65 mg, 0.5 mmol) in dichloromethane (50 mL) was added. The resulting mixture was stirred at rt for 6 h. The solvent was removed under reduced pressure and the resulting residue was purified by flash column chromatography (50% EtOAc/hexane) to afford Dansyl-DTTCP as yellow oil (2.25 g, 65%). The successful synthesis of Dansyl-DTTCP as fluorescent RAFT agent was confirmed by ^{1}H NMR characterization (**Figure S9**).

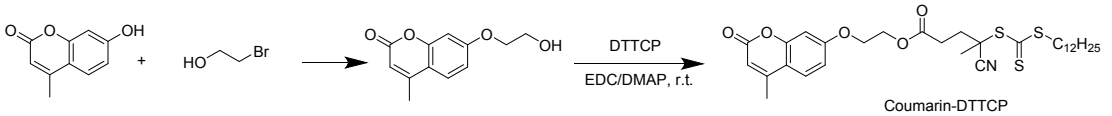

A suspension of 7-Hydroxy-4-methylcoumarin (4.00 g, 22.7 mmol) and potassium carbonate (6.23 g, 45.4 mmol) in dry DMF (40 mL) was stirred for 15 minutes. To the suspension, 2-bromoethanol (2.42 mL, 34.0 mmol) was added dropwise. After addition, the reaction was heated to 88 °C for 18 h under a nitrogen atmosphere. The reaction was cooled to room temperature and poured into iced water (150 ml). The solution was filtered and washed with H_2O (100 mL), the white precipitate was dried to obtain 7-(2-hydroxyethoxy)-4-methylcoumarin.[5]
To a solution of 7-(2-hydroxyethoxy)-4-methylcoumarin (1.10 g, 5.0 mmol) in dichloromethane (100 mL), a solution of DTTCP (2.0 g, 5.0 mmol), EDCI (3.83 g, 0.02 mol) and DMAP (65 mg, 0.5 mmol) in dichloromethane (50 mL) was added. The resulting mixture was stirred at rt for 6 h. The solvent was removed under reduced pressure and the resulting residue was purified by flash column chromatography (50% EtOAc/hexane) to afford Coumarin-DTTCP as yellow solid (1.76 g, 57%). The successful synthesis of Coumarin-DTTCP as fluorescent RAFT agent was confirmed by ^{1}H NMR characterization (**Figure S10**).

1.5 Preparations of Nucleobase-containing Polymers

General Procedure

In a Schlenk tube charged with the appropriate RAFT agent (0.05 mmol), AIBN (2 mg, 0.01 mmol) and the appropriate nucleobase-containing monomer (1.5 mmol) in DMSO (0.75 g), the suspension was carefully degassed by three freeze-evacuate-thaw cycles under high vacuum and then heated 70 ℃ for 12 h. After the polymerization, the nucleobase-containing polymer was isolated via precipitation into cold methanol (3 × 25 mL).

Poly(9-(4-vinylbenzyl)adenine) (P_sA) The title polymer was prepared according to the General Procedure using DTTCP (2 mg, 0.05 mmol) and 1-(4-vinylbenzyl)adenine (0.38 g, 1.50 mmol) to give P_sA (Scheme). GPC (DMF eluent) M_n 5500; M_w/M_n 1.23.

Poly(9-(4-vinylbenzyl)thymine) (P_sT)
The title polymer was prepared according to the General Procedure using DTTCP (2 mg, 0.05 mmol) and 1-(4-vinylbenzyl)thymine (0.37 g, 1.50 mmol) to give P_sT. GPC (DMF eluent) M_n 5700; M_w/M_n 1.24.

Poly(9-(4-vinylbenzyl)guanine) (P_sG)
The title polymer was prepared according to the General Procedure using DTTCP (2 mg, 0.05 mmol) and 9-(4-vinylbenzyl)guanine (0.43 g, 1.50 mmol) to give P_sG. GPC (DMF eluent) M_n 5600; M_w/M_n 1.25.

Poly(3-(cytosin-1-yl)propyl methacrylate) (P_mC)
The title polymer was prepared according to the General Procedure using DTTCP (2 mg, 0.05 mmol) and 3-(cytosin-1-yl)propyl methacrylate (0.36 g, 1.50 mmol), the polymer was isolated via precipitation into cold diethyl ether (3 × 25 mL) to give P_mC. GPC (DMF eluent) M_n 5400; M_w/M_n 1.27.
The successful synthesis of P_sA, P_sT, P_sG, P_mC were confirmed by ^{1}H NMR characterization (**Figure S11-S14**).
The polymerization process of fluorescent group-containing polymers (Danysl-P_sA, Coumarin-P_sT, Danysl-P_sG, Coumarin-P_mC) was similar with the polymerization process mentioned above, just change the RAFT agent from DTTCP to Dansyl-DTTCP or Coumarin-DTTCP.

1.6 Preparations of Nucleobase-containing amphiphilic block copolymers

P_sA, P_sT, P_sG, P_mC were synthesized as the macro-RAFT agent. The solvent was removed under reduced pressure. Dried P_sA (0.275 g, 0.05 mmol) (or P_sT (0.285 g, 0.05 mmol), P_sG (0.28 g, 0.05 mmol), P_mC (0.27 g, 0.05 mmol)), N-isopropyl acrylamide (NIPAM) (0.22 g, 1.90 mmol), AIBN (0.002 g, 0.01 mmol) and DMSO (0.96 g) were added to a 10 ml Schlenk tube. The mixture was degassed with three freeze-pump thaw cycles. The Schlenk tube was then immersed in an oil bath at 70 °C for 10 h. After the polymerization, the nucleobase-containing amphiphilic block copolymer P_sA-*b*-PNIPAM, P_sT-*b*-PNIPAM, P_sG-*b*-PNIPAM, P_mC-*b*-PNIPAM were isolated via precipitation into cold diethyl ether (3 × 25 ml). The successful synthesis of P_sA-*b*-PNIPAM, P_sT-*b*-PNIPAM, P_sG-*b*-PNIPAM, P_mC-*b*-PNIPAM were confirmed by ^{1}H NMR characterization (**Figure S25-S28**).

1.7 Self-assemblies formed by nucleobase-containing amphiphilic block copolymers

P_sA-*b*-PNIPAM (8 mM) was dissolved in DMSO, added to the DMSO solution of P_sT-*b*-PNIPAM (8 mM), the mixing solutions was stirring overnight and then dropped slowly to phosphate-buffered aqueous solution at physiological pH 7.5. Others types of self-assemblies formed by P_sG-*b*-PNIPAM and P_mC-*b*-PNIPAM were also prepared in the similar way.
In comparative experiment, P_sA-*b*-PNIPAM (8 mM) was dissolved in DMSO, dropping slowly to phosphate-buffered aqueous solution at physiological pH 7.5 with stirring, then P_sT-*b*-PNIPAM (8 mM) (dissolved in DMSO) was also added to the phosphate-buffered aqueous solution which containing P_sA-*b*-PNIPAM.

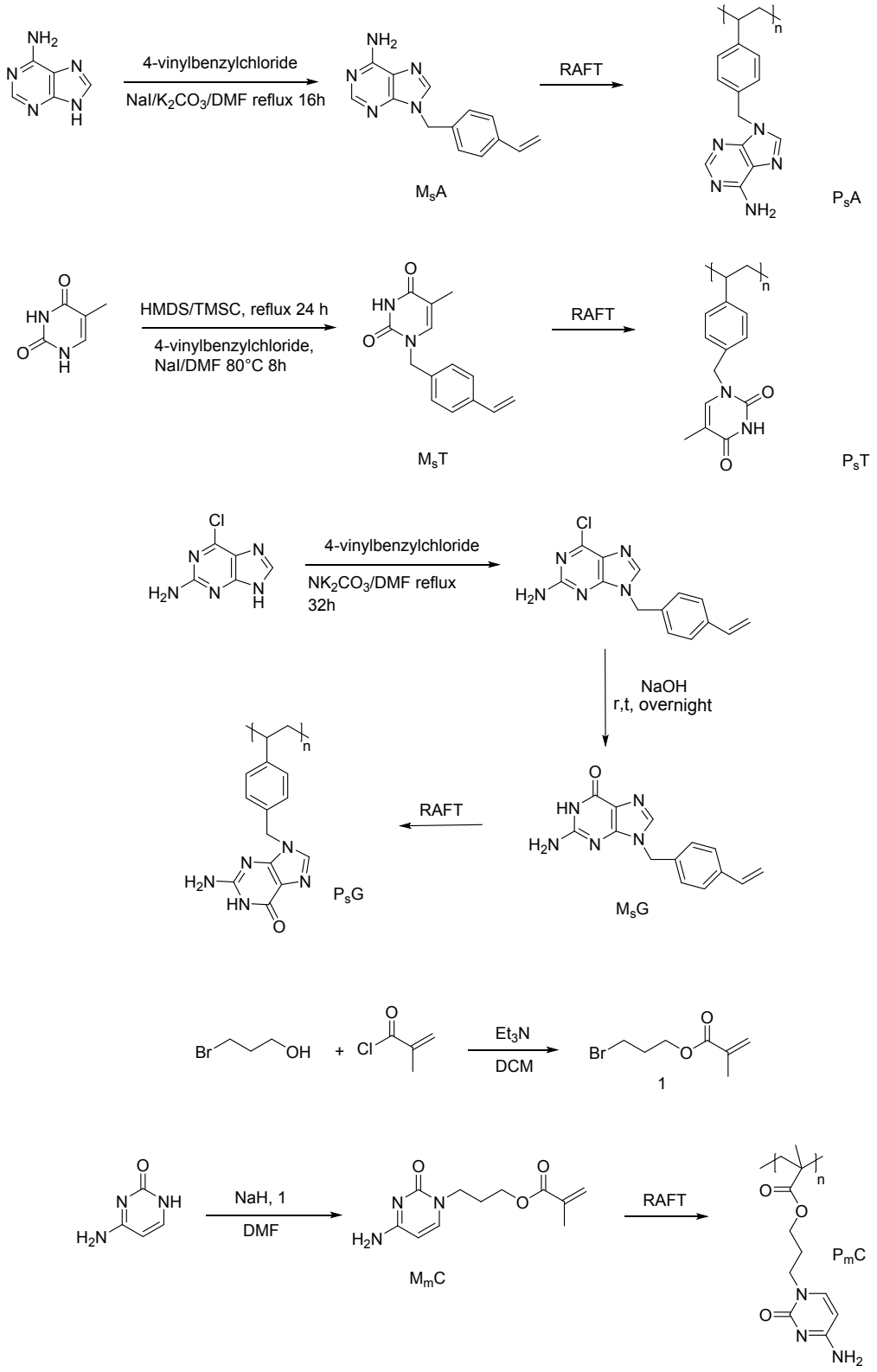

Scheme S1. The synthetic route of nucleobase-containing polymers.

Table S1. RAFT polymerization of nucleobase-functionalized monomers

Monomer	Polymer	M_n	$Đ$
M_sA	P_sA_{22}	5500	1.23
M_sT	P_sT_{24}	5700	1.24
M_sG	P_sG_{20}	5600	1.25
M_mC	P_mC_{22}	5400	1.27

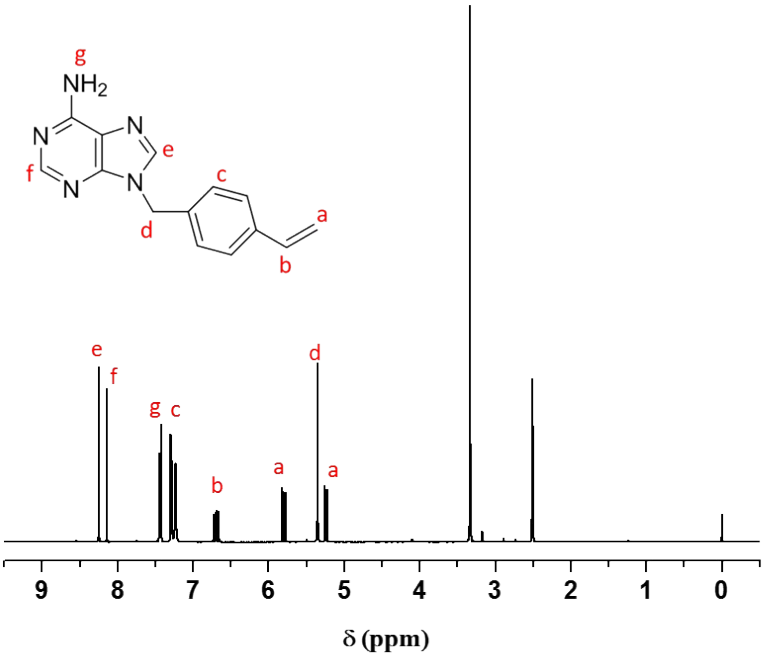

Figure S1. ^{1}H NMR spectrum of 9-(4-vinylbenzyl)adenine (M_sA) in DMSO-d_6.

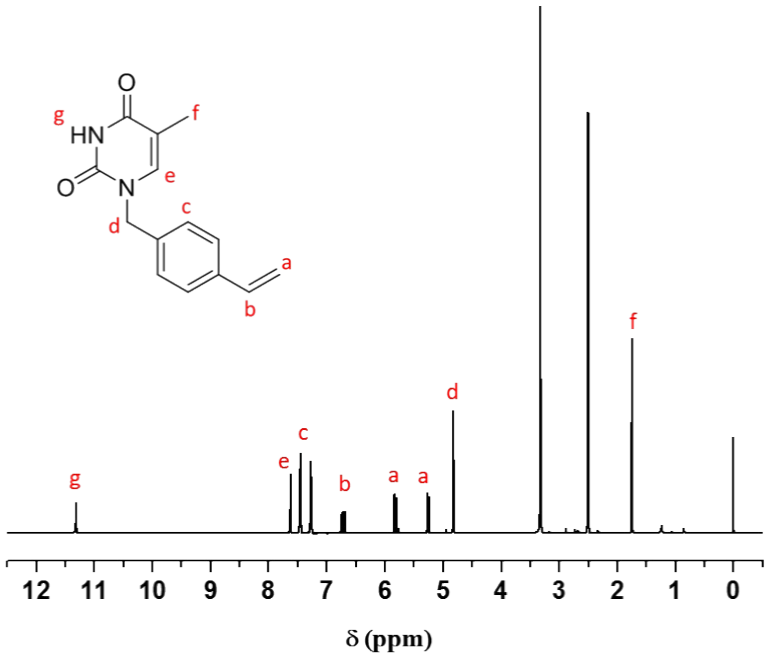

Figure S2. ^{1}H NMR spectrum of 1-(4-vinylbenzyl)thymine (M_sT) in DMSO-d_6.

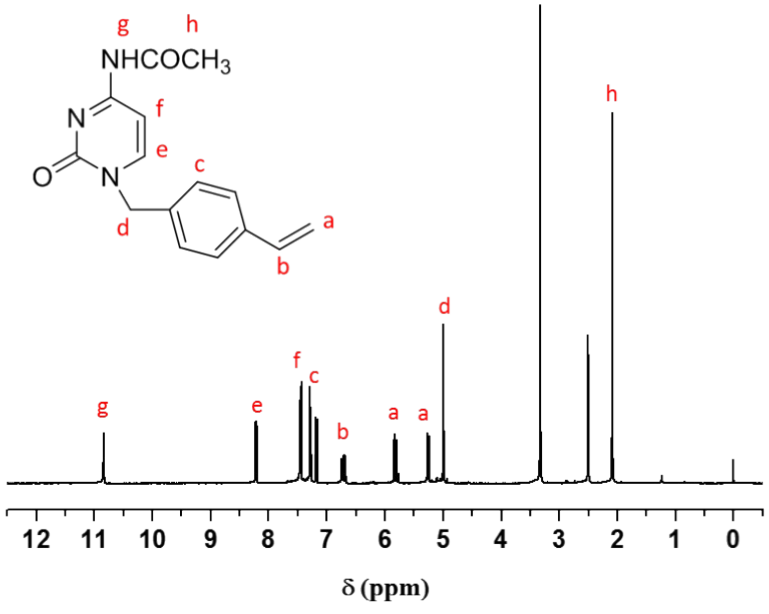

Figure S3. ^{1}H NMR spectrum of N-4-acetyl-1-(4-vinylbenzyl)cytosine in DMSO-d_6.

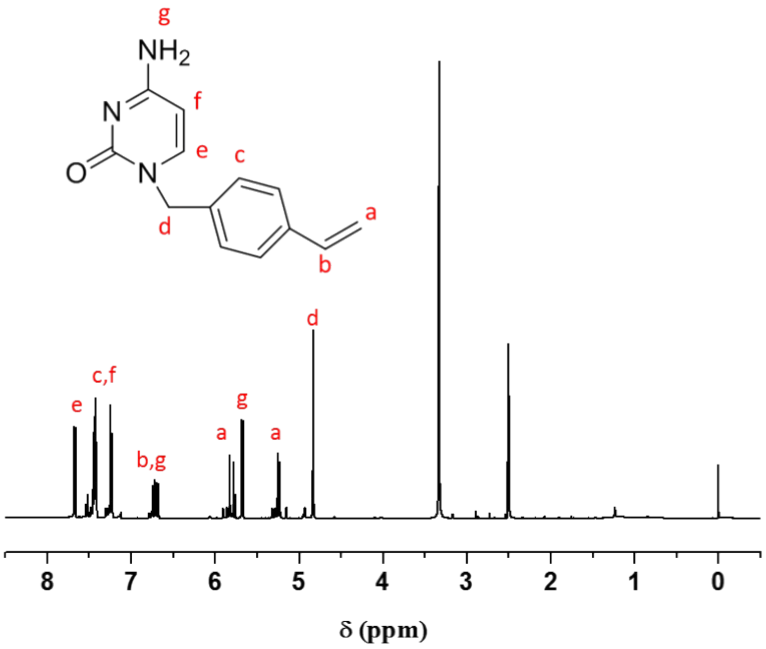

Figure S4. ^{1}H NMR spectrum of 1-(4-vinylbenzyl)cytosine (M_sC) in DMSO-d_6.

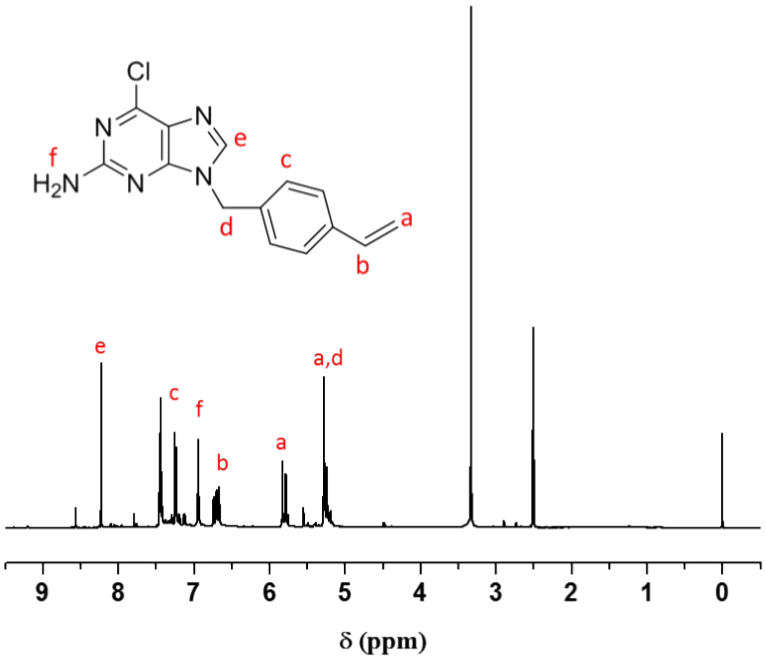

Figure S5. ^{1}H NMR spectrum of 2-amino-9-(4-vinylbenzyl)-6-chloro-9-H-purinein DMSO-d_6.

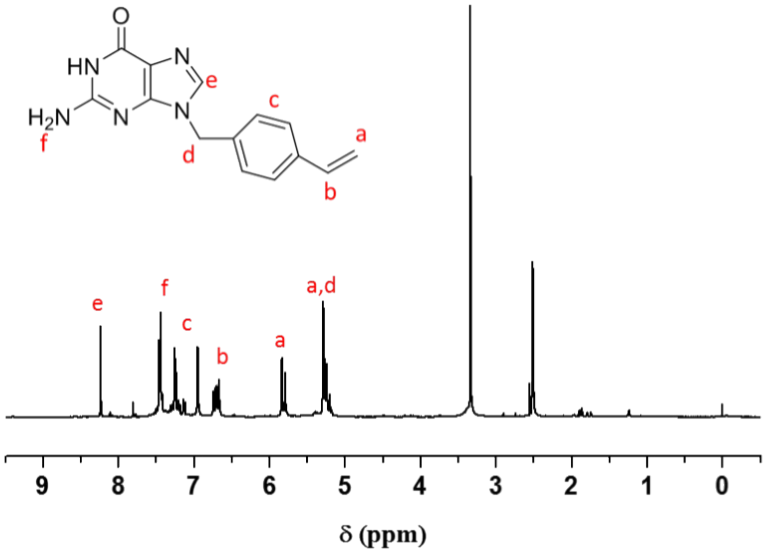

Figure S6. ^{1}H NMR spectrum of 9-(4-vinylbenzyl)guanine (M_sG) in DMSO-d_6.

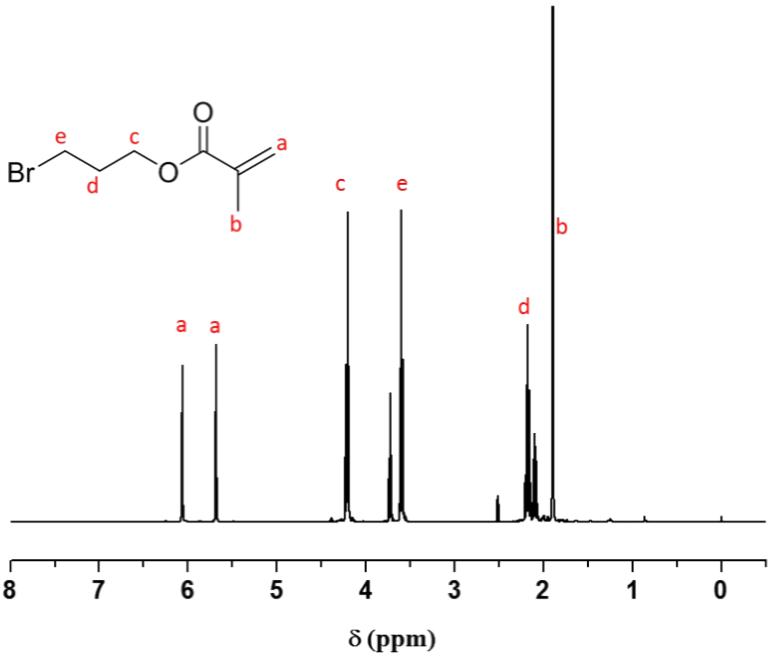

Figure S7. ^{1}H NMR spectrum of 3-bromopropyl methacrylate in DMSO-d_6.

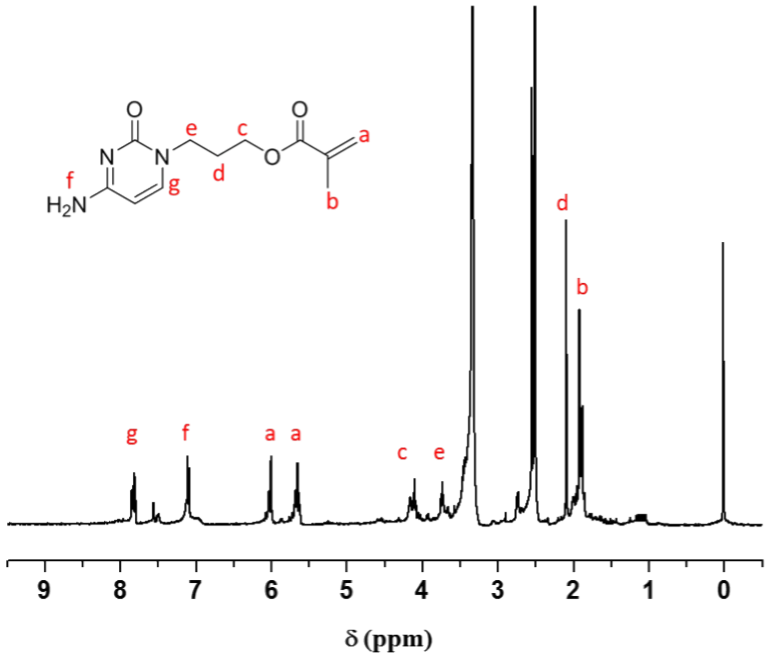

Figure S8. ^{1}H NMR spectrum of 3-(cytosin-1-yl)propyl methacrylate (M_mC) in DMSO-d_6.

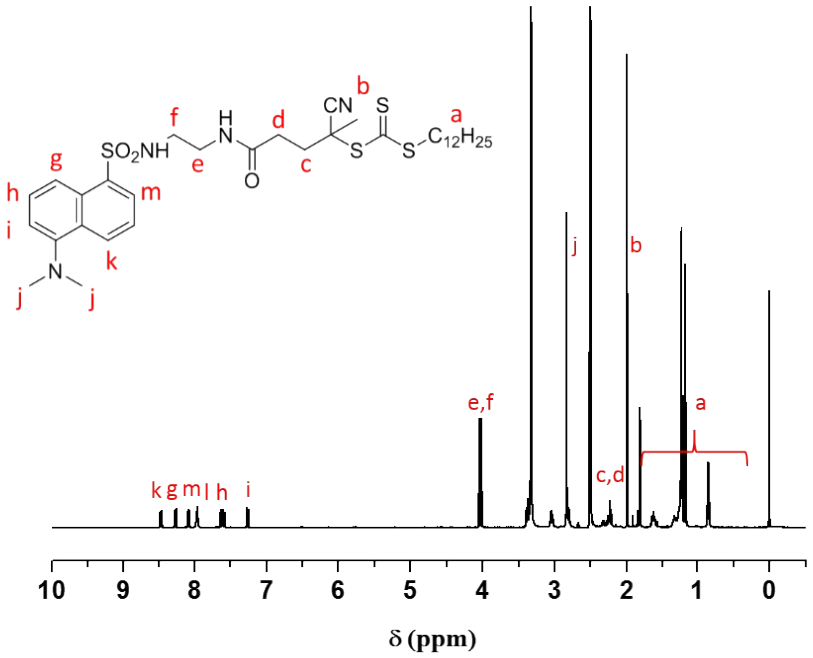

Figure S9. ^{1}H NMR spectrum of Dansyl-DTTCP in DMSO-d_6.

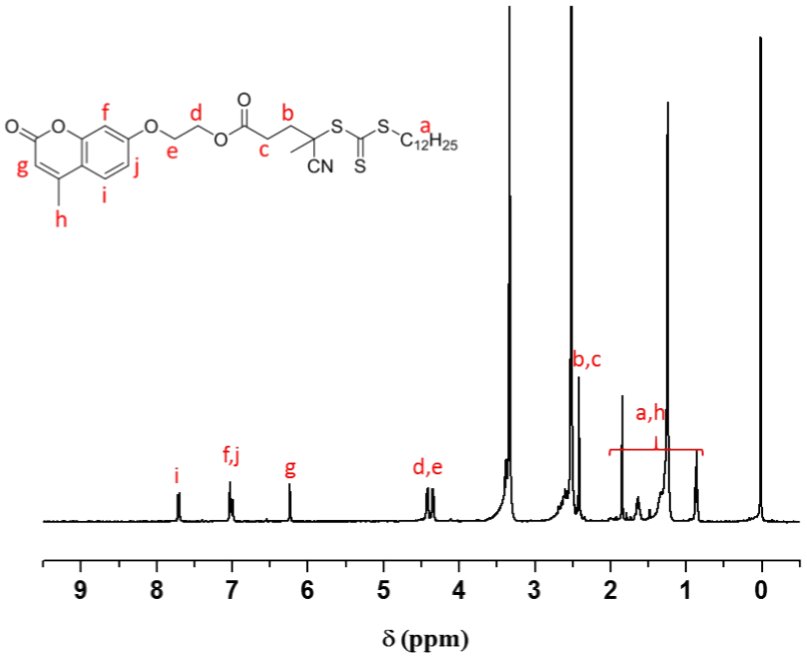

Figure S10. ^{1}H NMR spectrum of Coumarin-DTTCP in DMSO-d_6.

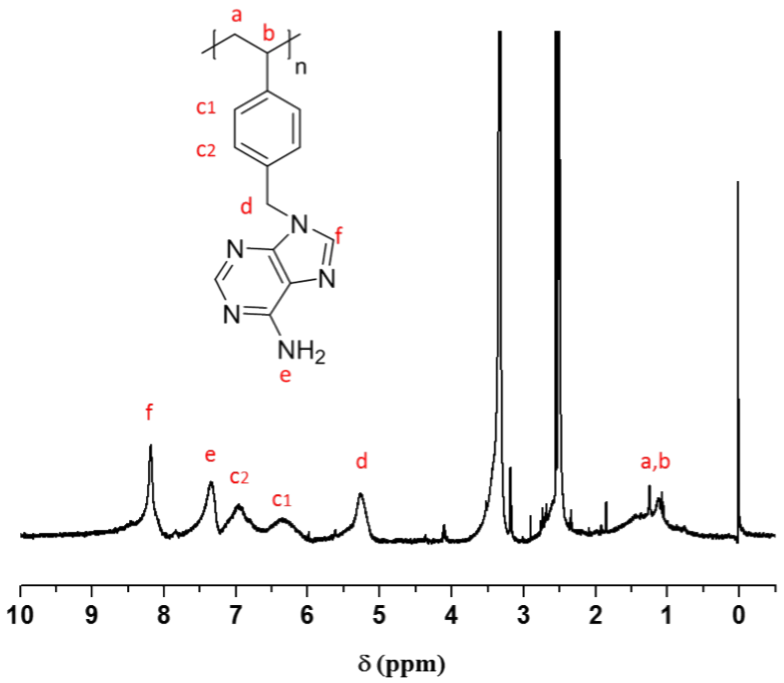

Figure S11. ^{1}H NMR spectrum of poly(9-(4-vinylbenzyl)adenine) (P_sA) in DMSO-d_6.

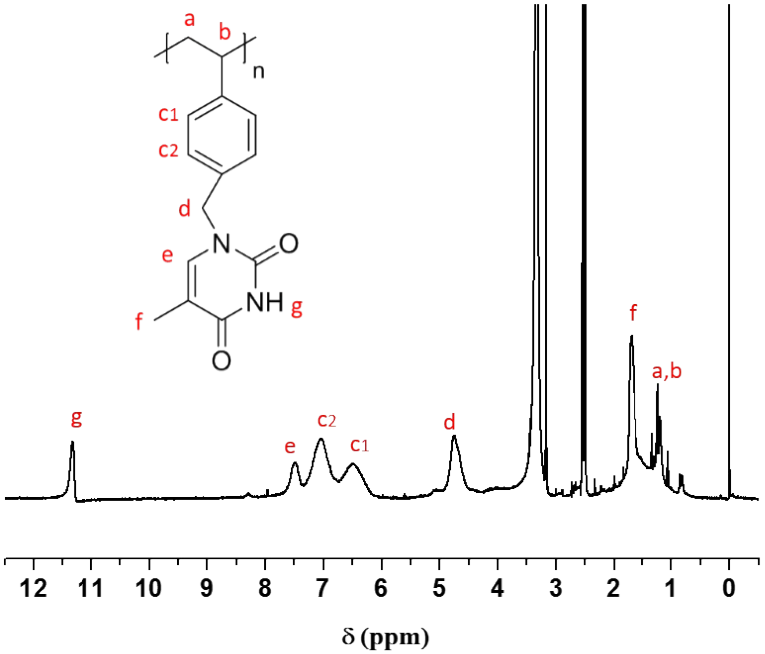

Figure S12. ^{1}H NMR spectrum of poly(1-(4-vinylbenzyl)thymine) (P_sT) in DMSO-d_6.

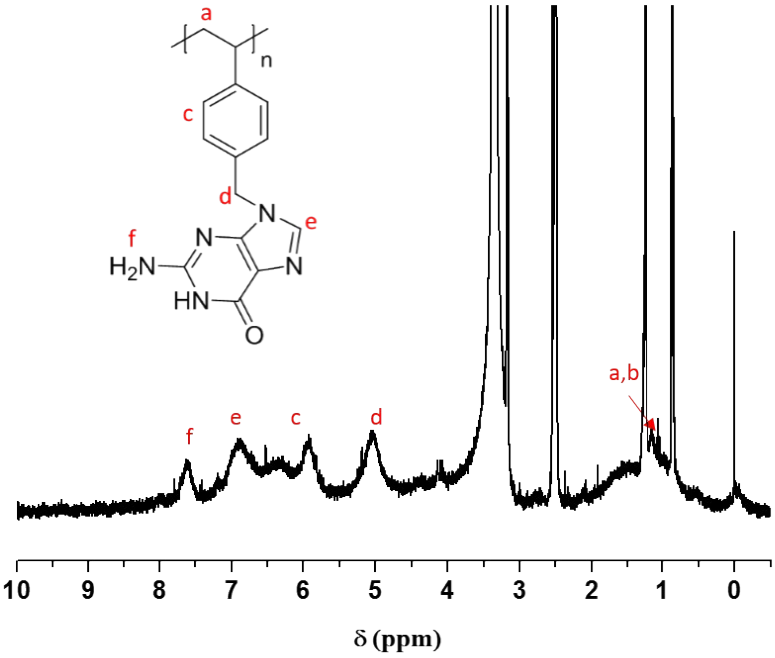

Figure S13. ^{1}H NMR spectrum of poly(9-(4-vinylbenzyl)guanine) (P_sG) in DMSO-d_6.

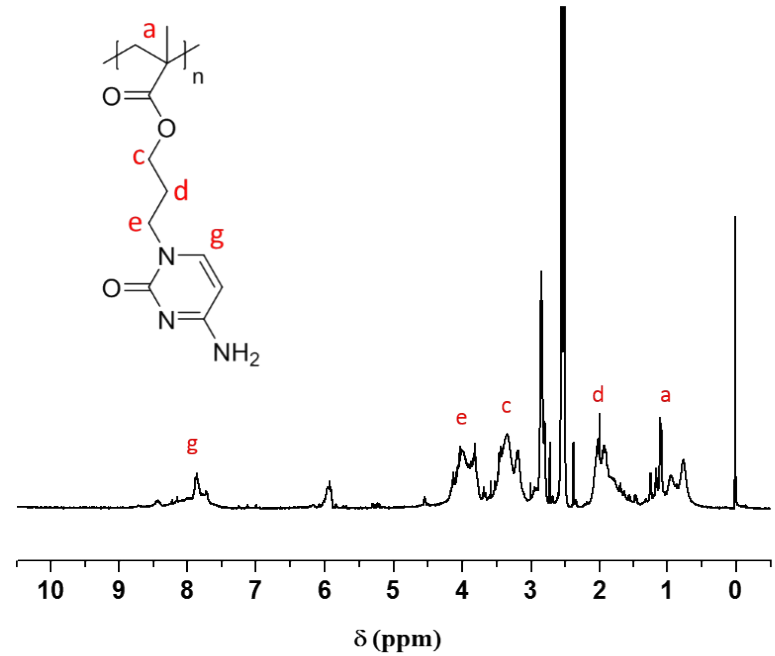

Figure S14. ^{1}H NMR spectrum of poly(3-(cytosin-1-yl)propyl methacrylate) (P_mC) in DMSO-d_6.

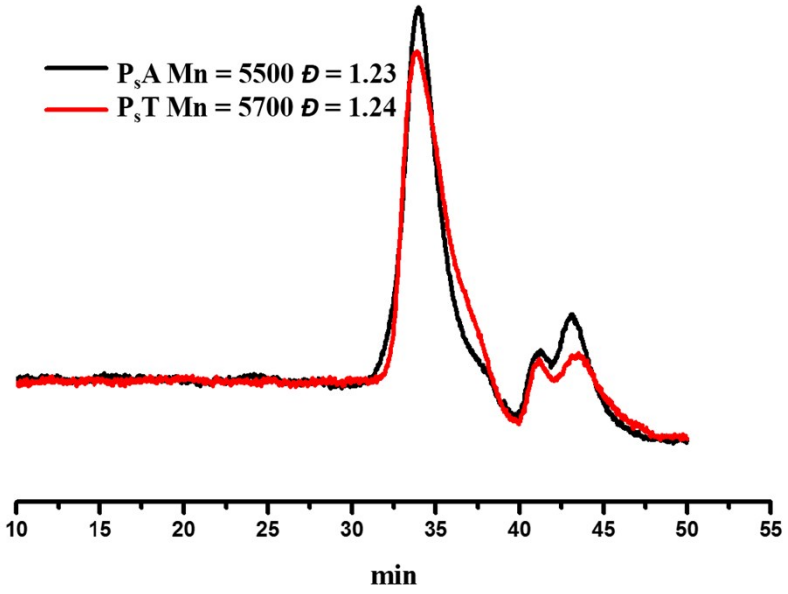

Figure S15. GPC (DMAc) traces of P_sA and P_sT.

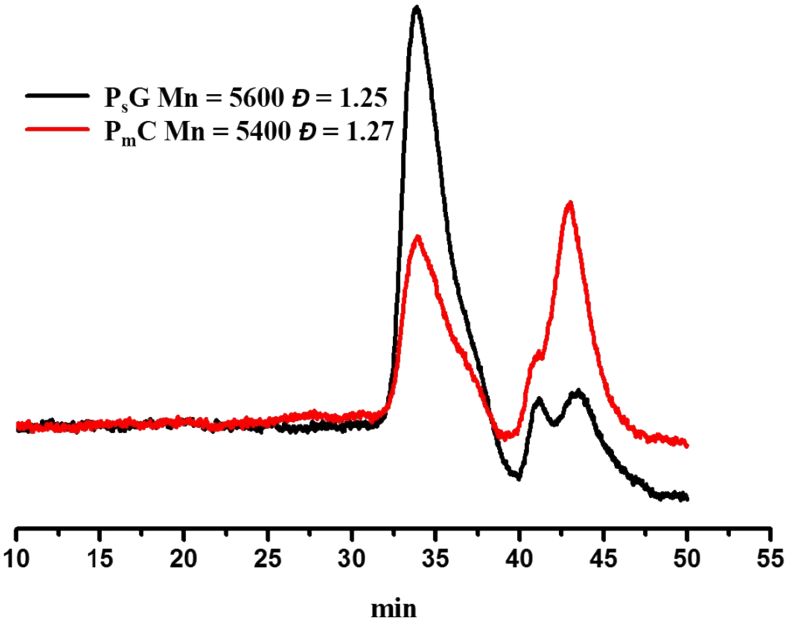

Figure S16. GPC (DMAc) traces of P_sG and P_mC.

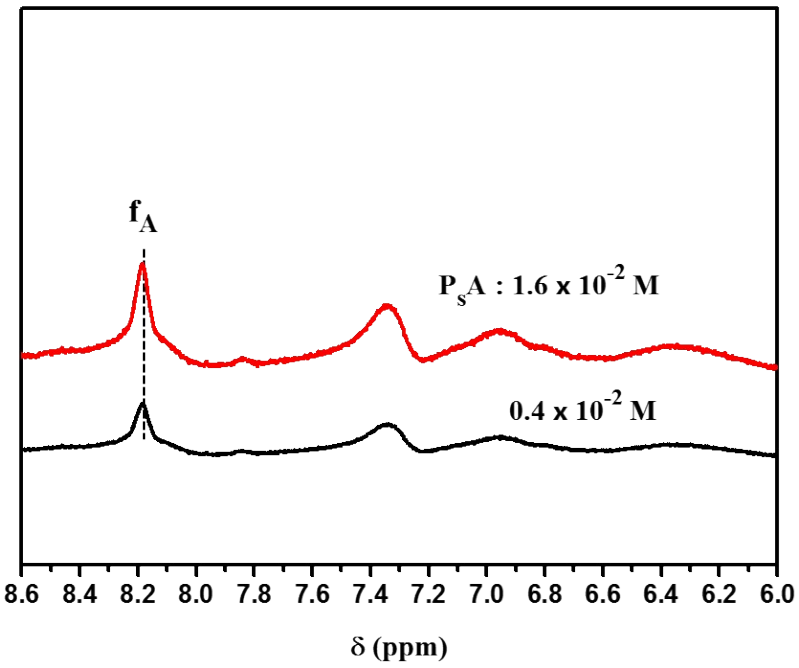

Figure S17. ^{1}H NMR spectrum of P_sA without P_sT in DMSO-d_6 at different concentrations.

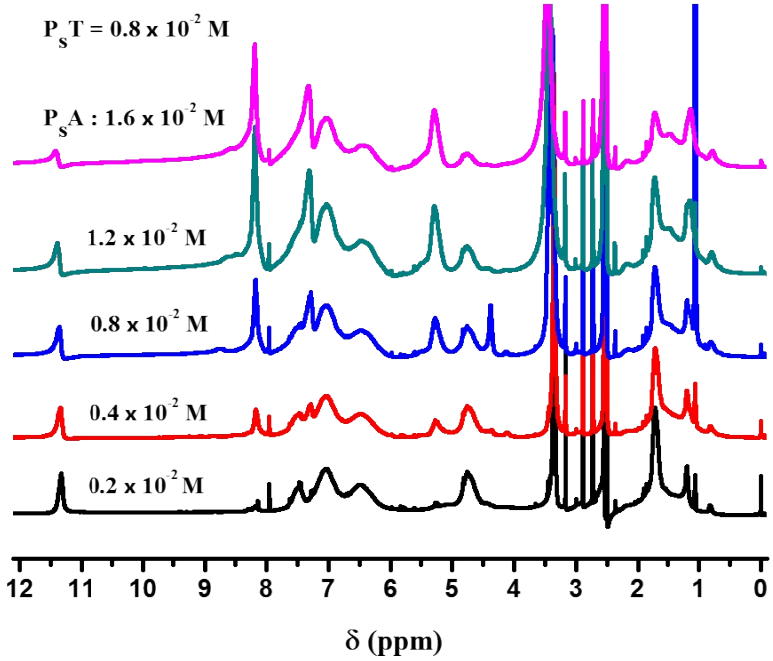

Figure S18. ^{1}H NMR spectrum of P_sA that bind P_sT in DMSO-d_6 at different concentrations.

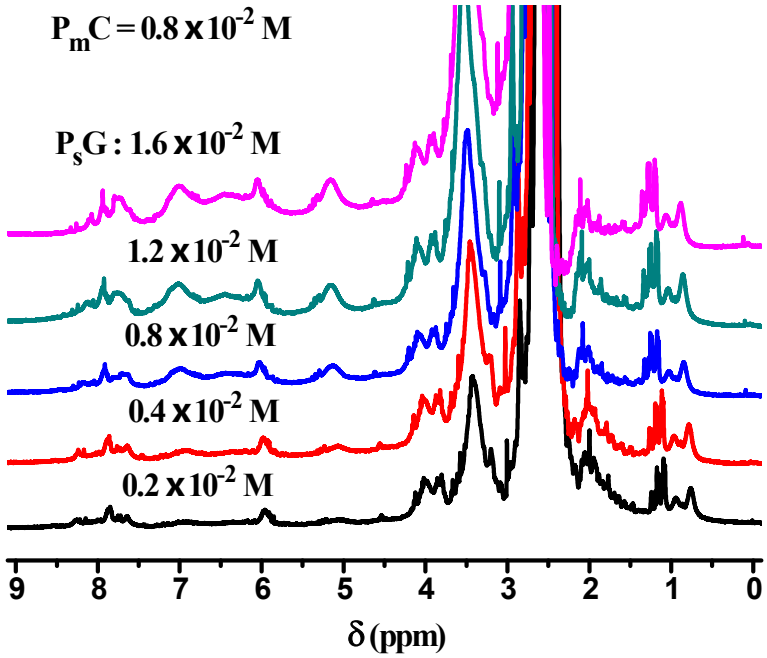

Figure S19. ^{1}H NMR spectrum of P_sG that bind P_mC in DMSO-d_6 at different concentrations.

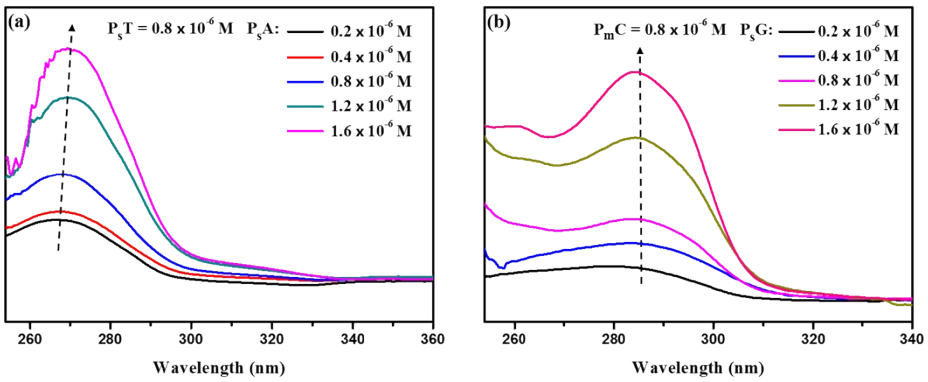

Figure S20. UV spectra of (a) P_sA bind P_sT and (b) P_sG bind P_mC at different concentrations.

In order to support our findings from ^{1}H NMR spectroscopy, UV-vis spectroscopy was utilized to confirm base-stacking interactions between P_sA bind P_sT and P_sG bind P_mC at different concentrations (**Figure S20**). The concentration of P_sT and P_mC was maintained at 0.8×10^{-6} M. In **Figure S20a**, with the increase in concentration of P_sA from 0.2×10^{-6} M to 1.6×10^{-6} M, the peak of P_sA shifts from 265 to 272 nm (red shift). When P_sA and P_sT bind together to form a complex, the aromatic rings from the polystyrene backbone interact with each other through base-stacking increasing the conjugation of the complex. The red shift observed in **Figure S20a** is a good indication of base-stacking interaction between P_sA and P_sT. In order to demonstrate the change in wavelength was a result of the base-stacking between P_sA bind P_sT, and not a result of the change in the concentration of P_sA,

a series of control experiments without adding P_sT in the system were investigated. As shown in **Figure S21**, it could be seen that the difference of concentration did not lead to a change in wavelength. This was further indication that there was base-stacking between P_sA bind P_sT. In **Figure S20b**, we did not observe a shift in wavelength of P_sG bind P_mC at different concentrations. Although P_sG contained a benzene moiety, P_mC did not contain an aromatic backbone, when they formed a complex, there were no base-stacking interactions involved. So no shift was observed in the UV-Vis spectrum (**Figure S20b).**

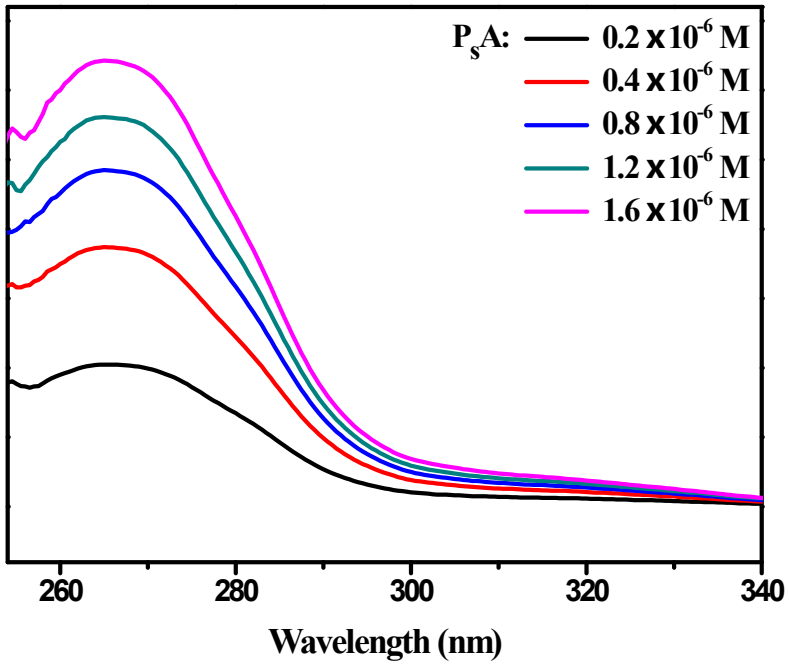

Figure S21. UV spectra of P_sA without P_sT at different concentration.

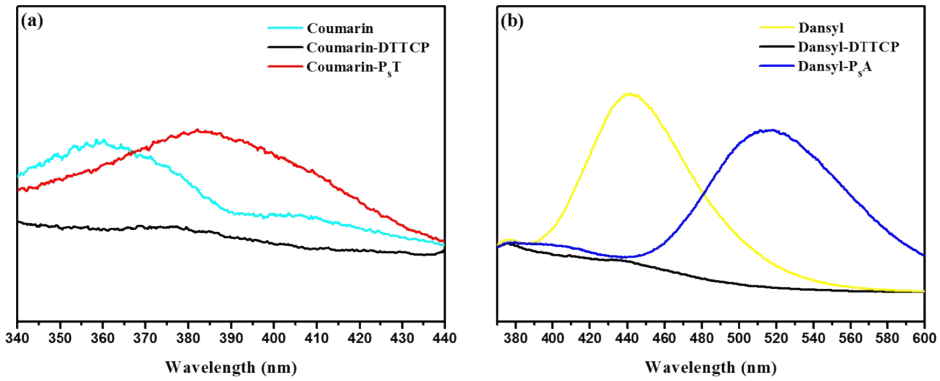

Figure S22. Fluorescence spectra of (a) coumarin, coumarin-DTTCP, coumarin-P_sT (C_F-P_sT) and (b) dansyl, dansyl-DTTCP, dansyl-P_sA (D_F-P_sA).

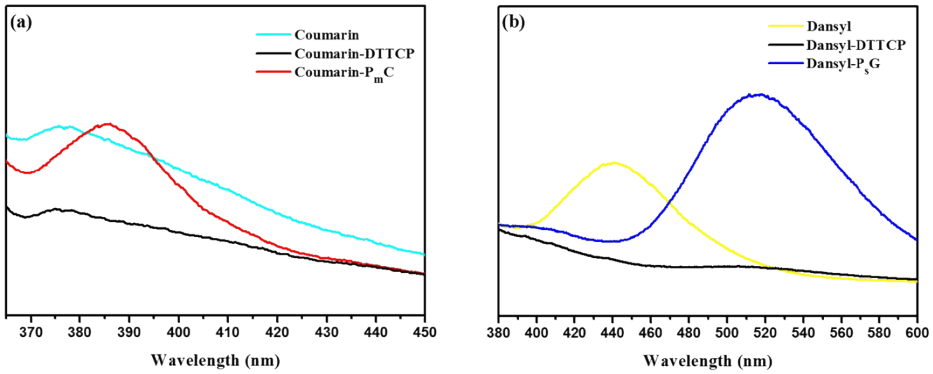

Figure S23. Fluorescence spectra of (a) coumarin, coumarin-DTTCP, coumarin-P_mC (C_F-P_mC) and (b) dansyl, dansyl-DTTCP, dansyl-P_sG (D_F-P_sG).

In **Figure S22**, the emission peak at 360 nm observed in coumarin is not observed in the RAFT agent coumarin-DTTCP due quenching of the fluorescence by the disulfide bond in the RAFT agent (**Figure S22a**). We observed the reappearance of the coumarin peak in coumarin-P_sT (C_F-P_sT), the rationale behind this phenomenon is due to the insertion of the monomers, the proximity of the coumarin moiety and DTTCP moiety increases and the disulfide bond in the RAFT agent no longer quenches the fluorescence of the coumarin. The emission wavelength of C_F-P_sT appeared at 382 nm, compared with the emission peak of coumarin at 360 nm. The shift in the peak is attributed to the extra conjugation in the nucleobase-containing polymer tethered to coumarin. A clear fluorescence emission peak of dansyl at 440 nm was observed in **Figure S22b**. As with coumarin, when dansyl is tethered to DTTCP, the fluorescence was quenched by the disulfide bond, while after the polymerization, the emission peak of dansyl-P_sA (D_F-P_sA) at 520 nm was observed. The shift of emission wavelength was also due to the aromatic rings in P_sA leading to a larger conjugated system. The fluorescence spectra of coumarin-P_mC (C_F-P_mC) and dansyl-P_sG (D_F-P_sG) are similar to C_F-P_sT and D_F-P_sA.

In **Figure S23**, contacted coumarin to DTTCP (coumarin-DTTCP), the emission peak of coumarin was disappear, it was due the disulfide bond on the DTTCP leaded to fluorescence quenching. Noted that the emission peak of coumarin-P_mC (C_F- P_mC) at 385 nm appeared again as a result of inserting monomers between disulfide bond and fluorescent group, the distance between them farther away, so the effect of disulfide bond to fluorescent group became weaker. Same as coumarin, when dansyl contacted to DTTCT, fluorescence was quenched by disulfide bond, while after the polymerization, the emission peak of dansyl-P_sG (D_F-P_sG) appeared again. The shift of emission wavelength was because of the benzene rings in P_sG had leaded to a bigger conjugated system.

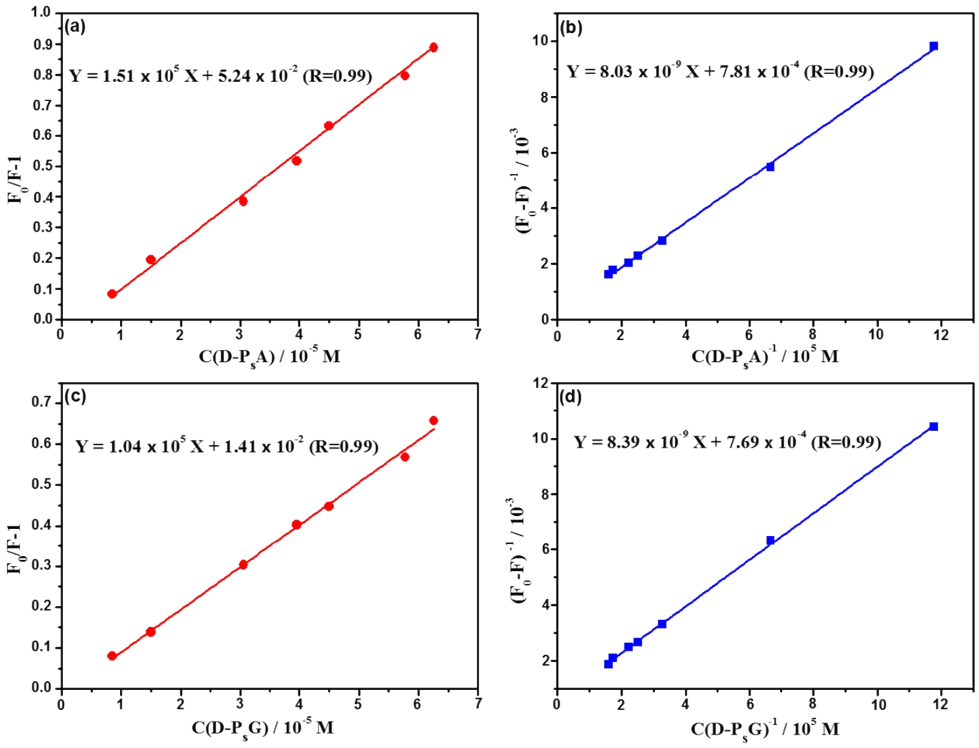

Figure S24. Quenching rate constant and binding constant of D_F-P_sA bind C_F-P_sT (a, b) and D_F-P_sG bind C_F-P_mC (c, d).

The quenching constants kq was determined by the Stern-Volmer equation (**eq. 1**),

$$F_0/F = 1 + k_q\tau_0[Q] \quad (1)$$

where F_0 was the fluorescence intensity in the absence of a quencher, F was the fluorescence intensity in the presence of a quencher and τ_0 is the fluorescence lifetime in the absence of a quencher.[6-8] In these two systems, the quencher was D_F-P_sA and D_F-P_sG.

For static quenching, the binding constant k_b could be calculated by using the Lineweaver- Burk plot (**Figure S24b, S24d, eq 2**), [6-8]

$$(F_0\text{-}F)^{-1} = F_0^{-1} + k_d^{-1}F_0^{-1}[Q]^{-1} \quad (2)$$

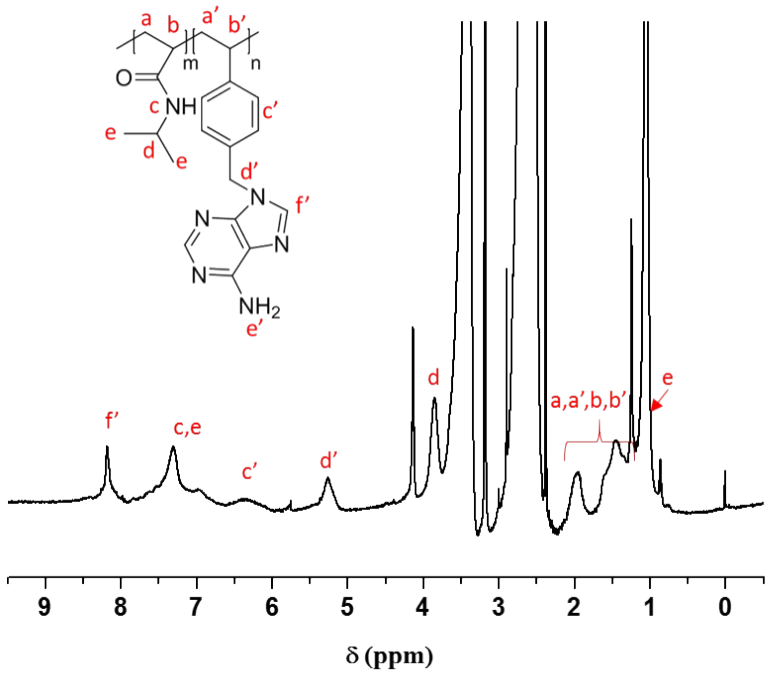

Figure S25. ^{1}H NMR spectrum of P_sA-*b*-PNIPAM in DMSO-d_6.

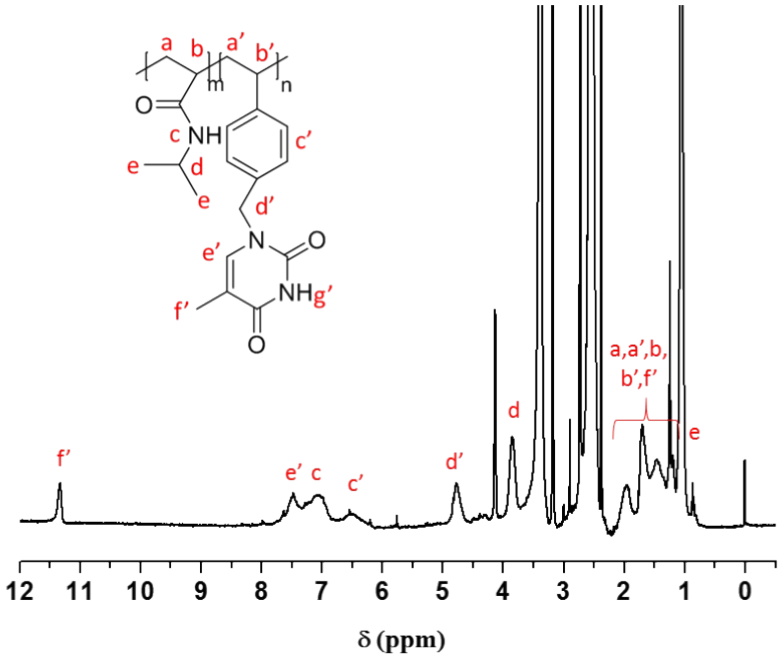

Figure S26. ^{1}H NMR spectrum of P_sT-*b*-PNIPAM in DMSO-d_6.

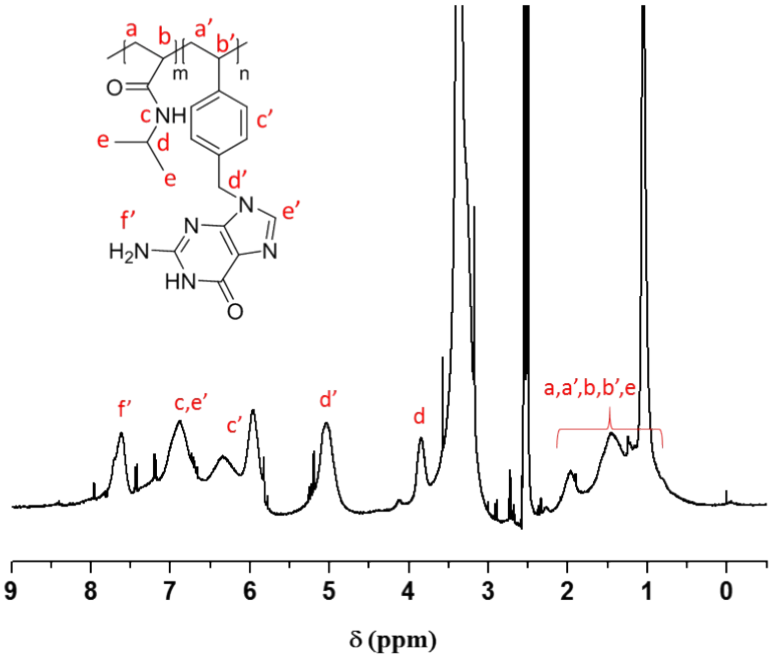

Figure S27. ^{1}H NMR spectrum of P_sG-*b*-PNIPAM in DMSO-d_6.

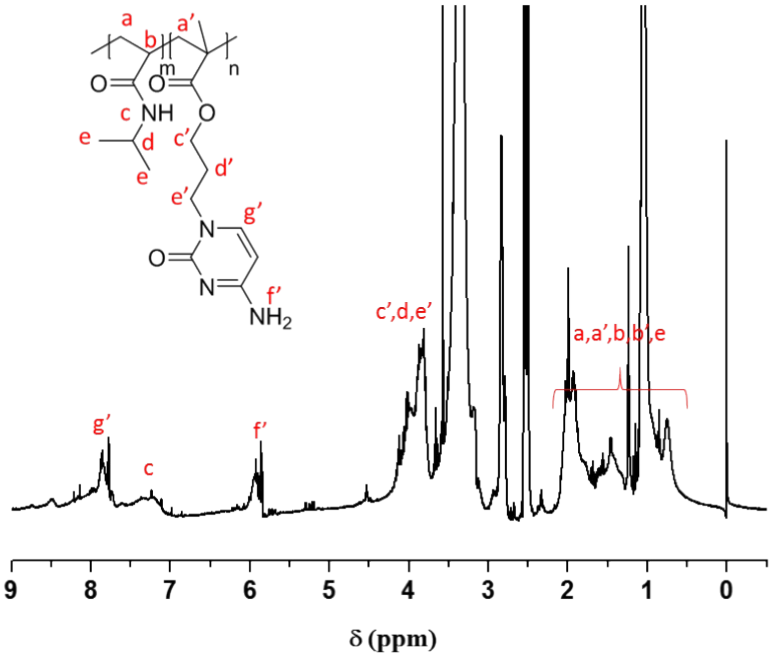

Figure S28. ^{1}H NMR spectrum of P_mC-*b*-PNIPAM in DMSO-d_6.

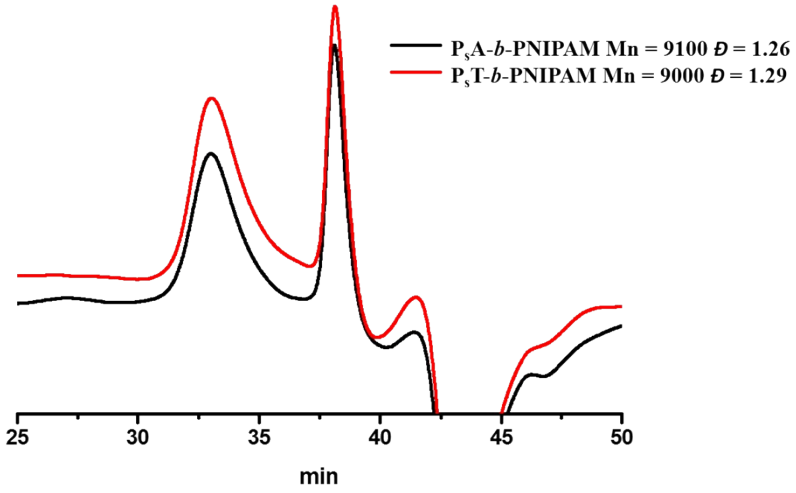

Figure S29. GPC (DMAc) traces of P$_s$A-*b*-PNIPAM and P$_s$T-*b*-PNIPAM.

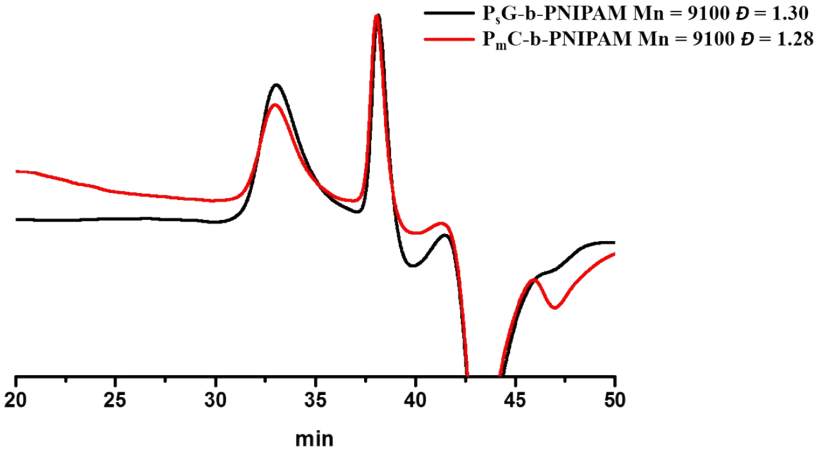

Figure S30. GPC (DMAc) traces of P$_s$G-*b*-PNIPAM and P$_m$C-*b*-PNIPAM.

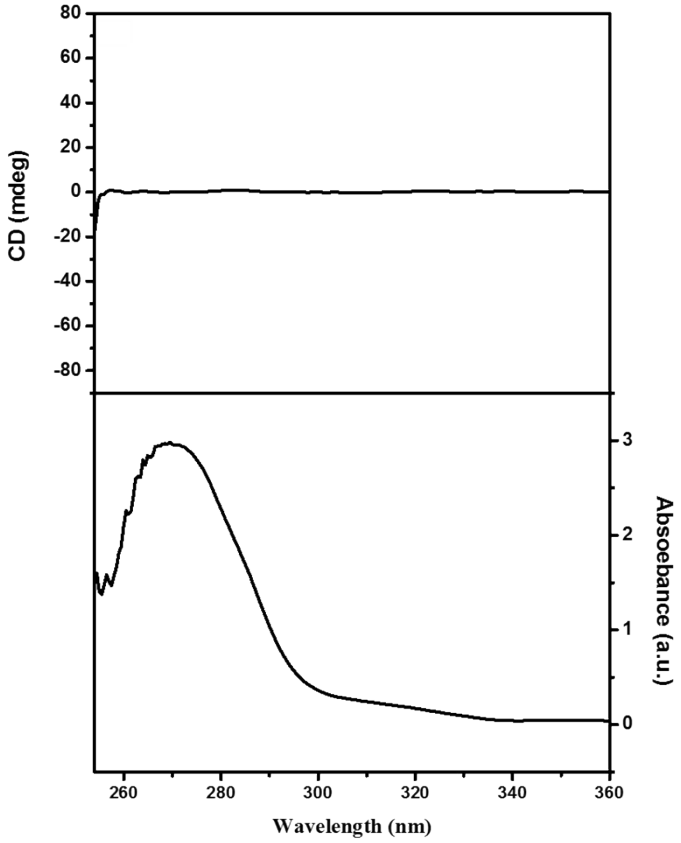

Figure S31. CD (up) and UV (down) spectra of P_sA bind with P_sT.

References

1. C. J. Ferguson, R. J. Hughes, B. T. Pham, B. S. Hawkett, R. G. Gilbert, A. K. Serelis and C. H. Such, *Macromolecules*, 2002, **35**, 9243-9245.
2. M. Sedlák, P. Šimůnek and M. Antonietti, *J. Heterocycl. Chem.*, 2003, **40**, 671-675.
3. H. J. Spijker, A. T. J. Dirks and J. C. van Hest, *Polymer*, 2005, **46**, 8528-8535.
4. C. Blaszykowski, S. Sheikh, P. Benvenuto and M. Thompson, *Langmuir*, 2012, **28**, 2318-2322.
5. S. Onbulak and J. Rzayev, *Poly. Chem.*, 2015, **6**, 764-771.
6. C. A. Seidel, A. Schulz and M. H. Sauer, *J. Phys. Chem. C*, 1996, **100**, 5541-5553.
7. Y. Ni, D. Lin and S. Kokot, *Talanta*, 2005, **65**, 1295-1302.
8. C. Kumar, R. Turner and E. Asuncion, *J. Photoch. Photobio. A*, 1993, **74**, 231-238.